Analysis of optical gain characteristics of Type-I InGaAsN/GaAs (Dilute N) based lasing nano-heterostructure

Syed Gulraze Anjum[1]*, Aboo Bakar Khan[1], Mohammad Jawaid Siddiqui[1], Parvez Ahmad Alvi[2]

[1]*Department of Electronics Engineering, ZHCET, Aligarh Muslim University, Aligarh, 202002, India*
[2]*Department of Physics, Banasthali University, Jaipur, 304022, India*

*Corresponding author

Abstract

In this article, we have computationally analyzed the Type-I InGaAsN/GaAs (dilute N) material system based step-index separately confined heterostructure (STINSCH) consisting of a compressively strained single quantum well layer. The whole structure is assumed to be grown on GaAs substrate. The optical gain spectra have been calculated and compared for single quantum well structure for the two different carrier densities under TE and TM polarization modes at room temperature. The size of the STINSCH based nano-scale heterostructure taken as a whole including SQW together with barriers and claddings is 47nm. In order to validate the computed optical gain, the anti-guiding factor has also been evaluated for the same nano-heterostructure. The GAIN software package has been utilized to obtain the various lasing properties like optical gain, modal gain, and anti-guiding factor. Therefore, this lasing nano-heterostructure may found application in optical fiber communication systems as a light source because of less attenuation and minimum optical loss. Copyright © 2018 VBRI Press.

Keywords: SQW lasing heterostructure, optical gain, InGaAsN/GaAs (dilute N), STINSCH.

Introduction

A most recent challenge for semiconductor devices is to develop advanced materials for the next generation of optical fiber communication systems. Recently, extensive research has discovered that an introduction of only a small percentage of nitrogen into III-V compound semiconductor lattice leads to a dramatic band gap reduction. This invention has opened the opportunity of utilizing these material systems for making semiconductor laser of desired wavelength range [1-4]. It is most of the time found beneficial to have electronic energy band gap engineering in several solid-state device applications, such as transistors, solar cells and semiconductor lasers. A heterojunction is an interface that occurs between two layers of unequal bandgap semiconducting materials. The combination of several heterojunctions collectively in a device is called a heterostructure. In 1963, a prominent scientist Herbert Kroemer recommended that population inversion could be greatly increased by including heterostructure in semiconductor lasers [5]. For producing more effective lasing action, a unique technique utilizes to make an especially thin active region (in 4nm-20nm range) [6, 7]. Those devices are called QW laser diodes. The major benefits of the quantum well based semiconductor laser are better output beam confinement, more efficient current-to-light conversion efficiency, the ability to emit a variety of wavelengths.

These benefits of quantum well structure drastically lessen the threshold current and enhance the possibility of varying emitting wavelengths by just changing the active layer thickness [8]. Quantum well based semiconductor lasers are existing with the following configurations, on the basis of quantum well numbers such as Single quantum well (SQW), Multiple quantum well (MQW) and on the basis of refractive index profile such as Step index separate confinement heterostructure (STINSCH), Graded index separate confinement heterostructure (GRINSCH). The new GaInNAs material attracts researcher most to overcome the poor temperature characteristics of usual long-wavelength laser diodes utilized for optical fiber communication systems [9]. Yong *et. al.* have thoroughly studied the optical gain of three different challenging active layer materials, i.e. InGaAsN–GaAs, AlGaInAs–AlGaInAs, and InGaAsP–InGaAsP [10]. Tomic *et. al.* have compared the gain properties of a standard InGaAsN/GaAs quantum well laser structure radiating at 1.3 µm with the similar N-free InGaAs/GaAs structure [11]. The room temperature CW operation of a GaInNAs–GaAs SQW laser diode with broad stripe geometry has already been demonstrated [12]. GaInNAs based dilute nitride lasers are considered to be promising light sources for upcoming optical fiber communication systems radiating at 1.3µm wavelength [13].

Structural and theoretical details

The suggested SCH based lasing nano-heterostructure comprises of a QW layer of $In_yGa_{1-y}As_xN_{1-x}$ material having a thickness of 70 A°, are placed between two wide bandgap barrier layers of GaAs material having a thickness of 100 A° followed by cladding layers of $Al_{0.4}Ga_{0.6}As$ material of 100 A° thickness. Clearly, the quantum well layer bandgap is narrower as compared to that of barrier region and barrier layer bandgap is narrower as compared to that of the cladding region. The schematic layer and band energy diagrams of a normal five layer lasing nano-heterostructure which consists of an SQW layer, two SCH layers, and two cladding layers for laser structure of InGaAsN/GaAs (Dilute N) material system can be seen in **Fig.1**. The prime aim of adding the cladding regions in the structure is to more effective light confinement as well as to lessen the series resistance so as to optimize the electrical and thermal resistivity in the proposed structure.

A 2% compressively strained single quantum well layer based semiconductor laser with a ridge width of 20μm and ridge length of 1000μm is simulated by utilizing GAIN software package. The strain amount is chosen in such a way to limit the level of energy bandgap in order to emit light in the desired wavelength range.

(a)

(b)
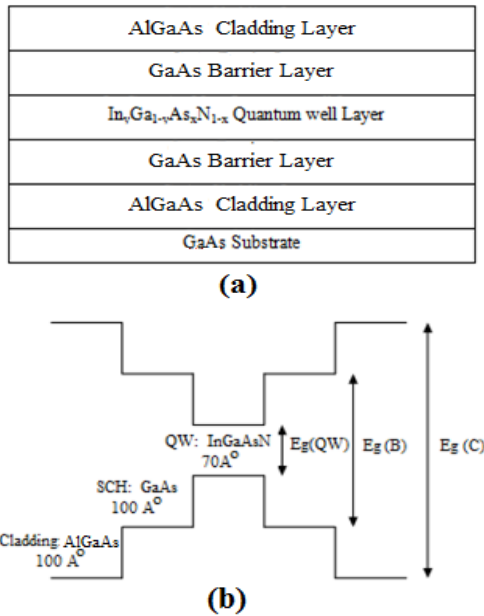
Fig. 1. Schematic (a) layer and (b) energy band diagrams.

The coefficient of optical gain for any material system varies with the photon energy and is expressed as follows:

$$G(E^{'}) = \frac{q^2|M_B|^2}{E^{'}\varepsilon_o m_o c \hbar n_{eff} W} \sum_{i,j} \int_{E_g}^{E_{gb}} m_{r,ij} C_{ij} A_{ij}[f_c - (1-f_v)]L(E)dE$$

where

q: Charge on an electron

$|M_B|^2$: Bulk momentum matrix element

E: Optical energy

ε_o : Vacuum permittivity

c : Speed of light in vacuum

n_{eff} : Effective refractive index

W : Quantum well width

i, j: Conduction and valence band quantum numbers

$m_{r,ij}$: The reduced effective mass

C_{ij} : The overlap factor

A_{ij} : The anisotropic factor

f_c , f_v : Fermi-Dirac distribution of the conduction and valence bands.

$L(E)$: Lorentzian lineshape function

Subsequently, an anti-guiding factor (α) which is a very important parameter and plays a very vital role in the heterostructure. It is calculated as

$$\alpha = -\frac{4\pi n'}{\lambda G'}$$

where G' and n' are defined as dG/dN (differential gain) and dn/dN (differential refractive index change), respectively [6, 7, 14].

Results and discussion

Optical gain as a function of lasing wavelength and photon energy in TE polarization mode for two different carrier concentrations of $2\times10^{18}/cm^3$ and $3\times10^{18}/cm^3$ have been investigated for the aforementioned lasing nano-heterostructure shown in **Fig. 2**.
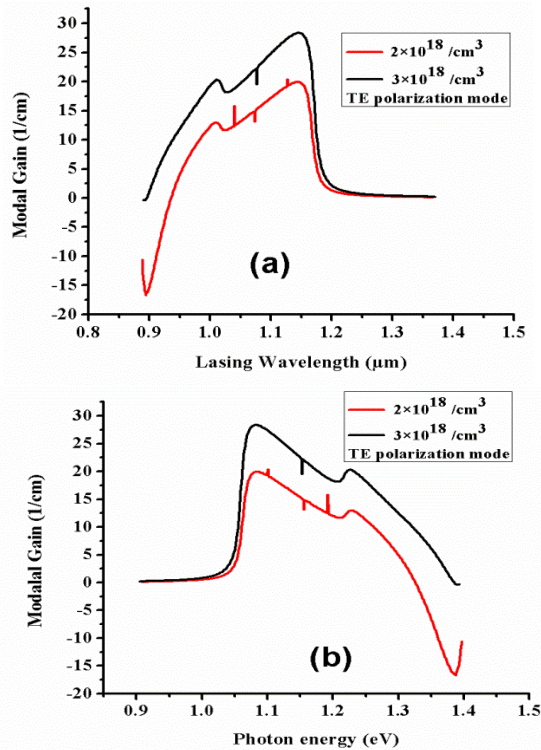

(a)

(b)
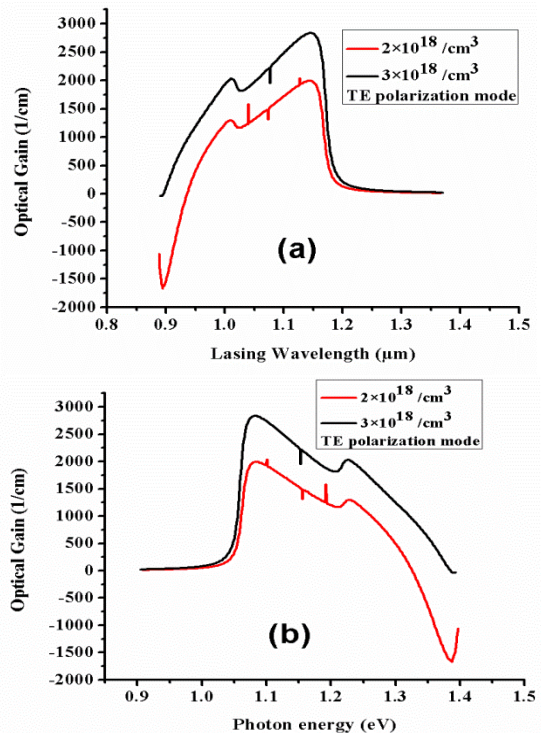
Fig. 2. Optical gain as a function of (a) wavelength (b) photon energy in TE polarization mode.

Modal gain as a function of lasing wavelength and photon energy in TE polarization mode for two different carrier concentrations of $2\times10^{18}/cm^3$ and $3\times10^{18}/cm^3$ have been thoroughly investigated as shown in **Fig. 3**.
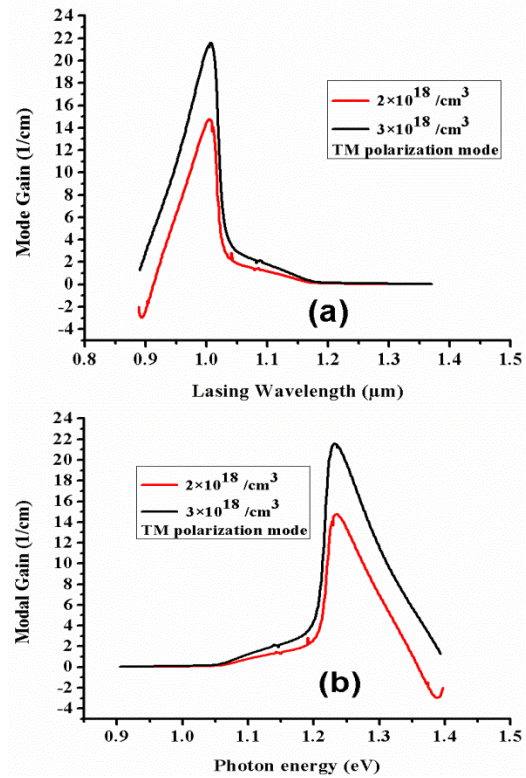

Fig. 3. Modal gain as a function of (a) wavelength (b) photon energy in TE polarization mode.

Fig. 4. Optical gain as a function of (a) wavelength (b) photon energy in TM polarization mode.

Optical gain as a function of lasing wavelength and photon energy in TM polarization mode for two different carrier concentrations of $2\times10^{18}/cm^3$ and $3\times10^{18}/cm^3$ have been explored as shown in **Fig. 4**.

Modal gain as a function of lasing wavelength and photon energy in TM polarization mode for two different carrier concentrations of $2\times10^{18}/cm^3$ and $3\times10^{18}/cm^3$ have been thoroughly analyzed as shown in **Fig. 5**.

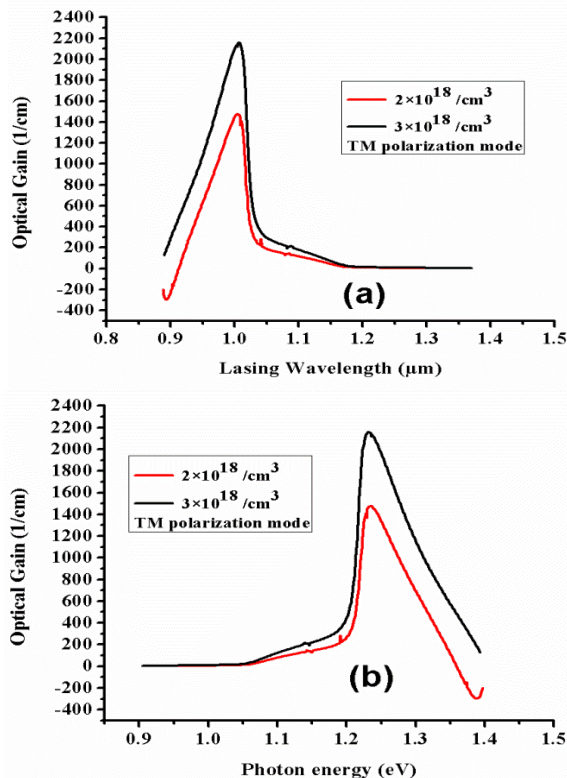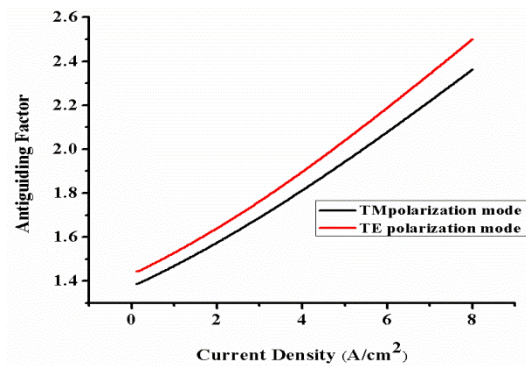**Fig. 5.** Modal gain as a function of (a) wavelength (b) photon energy in TM polarization mode.

Fig. 6. Anti-guiding factor as a function of current density.

The overall maximum optical gain of ~2800/cm is achieved at carrier concentration of $3\times10^{18}/cm^3$ in TE polarization mode. The simulations results agree well with the published experimental data. The anti-guiding factor has also been determined and is observed in between the range of 1.42 and 2.5 in TE mode of polarization .& in between 1.38 and 2.35 in TM mode of polarization as shown in **Fig. 6**.

Conclusion

The optical gain of TypeI InGaAsN/GaAs (Dilute N) based lasing nano-heterostructure on GaAs substrate has been theoretically studied under TE and TM polarization modes. The overall peak optical gain of ~2800/cm is obtained at ~1.15μm wavelength corresponding to the photonic energy of ~1.1eV at the carrier density of 3.0×10^{18} /cm^3 in TE polarization mode at room temperature. However, the obtained peak optical gain for Type-I InGaAsN/GaAs(Dilute N) based lasing nano-heterostructure in TE polarization mode is found larger as compared to that in TM polarization mode at the same carrier density. Therefore, the Type-I InGaAsN/GaAs(Dilute N) based lasing nano-heterostructure with the overall structural size of 47nm including 7nm well width may found application in the area of optical fiber communication systems as a light source.

References

1. Coleman, J. J.; *Semiconductor Science and Technology*, **2012**, *27,* 090207.
2. Chuang, S. L.; Physics of Optoelectronic Devices, John Wiley & Sons, Inc., **1995**.
3. Bhattacharya, P.; Semiconductor Optoelectronic Devices, Prentice Hall, NJ, USA, **1996**.
4. Mynbaev, D.K.; Scheiner, L.L.; Fiber-Optic Communications Technology. Prentice Hall, NJ, USA, **2001**.
5. Kroemer, H.; *IEEE Proceedings*, **1963**, *51,* 1782.
6. Lal, P.; Dixit, S.; Dalela S.; Rahman, F.; Alvi, P. A.; *Physica E*, **2012**, *46,* 224..
7. Kumari, V.; Ashish; Jha, S.; Rathi, A.; Nirmal, H. K.; Lal, P.; Alvi, P. A.; *Journal of Optoelectronics Engineering*, **2014**, 2, 42.
8. Anjum, S. G.; Siddiqui, M. J.; *IEEE Proceedings of International Conference on Multimedia, Signal Processing and Communication Technologies (IMPACT)*, **2013**.
9. Kondow, M.; Kitatani, T.; Nakatsuka, S.; Larson, M. C.; Nakahara, K.; Yazawa, Y.; Okai, M.; Uomi, K.; *IEEE Journal of Selected Topics Quantum Electronics*, **1997**, *3,* 719.
10. Yong, J. C.; Rorison, J. M.; White, I. H.; *IEEE Journal of Quantum Electronics*, **2002**, *38* (12), 1553.
11. Tomic, S.; O'Reilly, E. P.; *PHYSICA E* , **2002**, *13,* 1102.
12. Kitatani, T.; Kondow, M.; Nakatsuka, S.; Yazawa, Y.; Okai, M.; *IEEE Journal of Selected Topics in Quantum Electronics*, **1997**, *3, 2,* 206.
13. Jouhti, T.; Peng, C. S.; Pavelescu, E. M.; Konttinen, J.; Gomes, L. A.; Okhotnikov, O. G.; Pessa, M.; *IEEE Journal of Selected Topics in Quantum Electronics*, **2002**, *8, 4,* 787.
14. Yadav, R.; Lal, P.; Rahman, F.; Dalela, S.; Alvi, P. A.; International Journal of Modern Physics B, **2014**, *28,* 10.